Cosmological constraints in the presence of ionizing and resonance radiation at recombination

Rachel Bean,[1] Alessandro Melchiorri,[2] and Joseph Silk[3]

[1]*Dept. of Astronomy, Space Sciences Building, Cornell University, Ithaca, New York, USA*
[2]*Dipartimento di Fisica e sezione INFN, Universita' di Roma "La Sapienza", Ple Aldo Moro 2, 00185, Rome, Italy*
[3]*Astrophysics, Denys Wilkinson Building, University of Oxford, Keble Road, OX3RH, Oxford, United Kingdom*

(Received 12 January 2007; published 14 March 2007)

With the recent measurement of full sky cosmic microwave background (CMB) polarization from WMAP, key cosmological degeneracies have been broken, allowing tighter constraints to be placed on cosmological parameters inferred assuming a standard recombination scenario. Here we consider the effect on cosmological constraints if additional ionizing and resonance radiation sources are present at recombination. We find that the new CMB data significantly improve the constraints on the additional radiation sources, with $\log_{10}[\epsilon_\alpha] < -0.5$ and $\log_{10}[\epsilon_i] < -2.4$ at 95% c.l. for resonance and ionizing sources, respectively. Including the generalized recombination scenario, however, we find that the constraints on the scalar spectral index n_s are weakened to $n_s = 0.98 \pm 0.03$, with the $n_s = 1$ case now well inside the 95% c.l. The relaxation of constraints on tensor modes, scale invariance, dark energy and neutrino masses are also discussed.

DOI: 10.1103/PhysRevD.75.063505 PACS numbers: 98.80.Cq

I. INTRODUCTION

The recent measurements of the cosmic microwave background (CMB) flux provided by the 3 yr Wilkinson Microwave Anisotropy Probe (WMAP) mission (see [1–4] have confirmed several of the results already presented in the earlier data release, but also pointed towards new conclusions. The better treatment of systematics in large-scale polarization data, in particular, has now provided a lower value for the optical depth parameter τ. This, together with an improved signal in the temperature data at higher multipoles, has resulted in a lower value of the spectral index parameter $n_s = 0.959 \pm 0.016$. A determination of this parameter can play a crucial role in the study of inflation. Soon after the WMAP data release, several papers have indeed investigated the possibility of discriminating between single-field inflationary models by making use of this new, high quality, data set [5–13]. One of the main conclusions of these papers is that some inflationary models, such as quartic chaotic models of the form $V(\phi) \sim \lambda\phi^4$, may be considered ruled out by the current data while others, such as chaotic inflation with a quadratic potential $V(\phi) \sim m^2\phi^2$ are consistent with all data sets.

While the WMAP result is of great importance for inflationary model building, one should be careful in taking any conclusion as definitive since the constraints on n_s are obtained in an indirect way and are, therefore, model dependent. Similar considerations applies to other cosmological constraints, such those on the dark energy equation of state and neutrino masses. Combining CMB anisotropies with galaxy clustering and supernovae type Ia data, the dark energy equation of state parameter (dark energy pressure over density) has been constrained to $w = -1.08 \pm 0.12$ at 95% c.l. (see [1]). Using the same data set, but under the assumption of a cosmological constant, it is possible to constrain the neutrino masses to $\sum m_i < 0.66$ eV at 95% c.l. where $i = 1, \ldots, 3$ and indicates the neutrino flavor. Again, while those constraints play a very important role in our understanding of the dark energy component and neutrino physics, they are obtained in an indirect way and under several assumptions.

The importance of the model dependency of the cosmological constraints has been recently discussed by several authors. The impact of isocurvature modes on the determination of the neutrino mass [14], dark energy properties [15], scalar spectral index [16] and baryon density [17] is just one example.

Here we investigate possible deviations in the mechanism on which CMB anisotropies are highly dependent: the process of recombination.

In a previous paper [18], we analyzed modified recombination processes in light of the WMAP first year data. Here we assess the improvements given by more recent data, in particular, the inclusion of CMB polarization spectra, and also extend the analysis to a larger set of parameters. We will indeed not only provide new and more stringent constraints on modified recombination but we also consider its impact on inflationary, dark energy and neutrino parameters.

The recombination process can be modified in several ways. For example, one could use a model-independent, phenomenological approach such as in [19] where models are specified by the position and width of the recombination surface in redshift space. Here we instead focus on theoretically motivated mechanisms based on extra sources of ionizing and resonance radiation at recombination (see e.g. [20]). While the method we adopt will be general enough to cover most of the models of this kind, as discussed in the next section, we remind the reader that there exist other ways in which to modify recombination, for instance, by having a time-varying fine-structure constant [21].

Following the seminal papers [22,23] detailing the recombination process, further refinements to the standard scenario were developed [24], allowing predictions at the accuracy level found in data from the WMAP satellite and the future Planck satellite [25,26]. With this level of accuracy, it becomes conceivable that deviations from standard recombination maybe be detectable [20,27,28], although further refinements could be required to get the Thomson visibility function below percent level accuracy [29–31].

The paper proceeds as follows: in Sec. II we describe a model which can produce deviations from the standard recombination scenario. In Sec. III, we describe how these deviations might affect the CMB temperature and polarization power spectra and conduct a likelihood analysis using the recent CMB data from WMAP and other cosmological observables. In particular, we will study the impact that a modified recombination scheme can have on several cosmological and astrophysical parameters. In Sec. IV we draw together the implications of the analysis.

II. A MODIFIED IONIZATION HISTORY

The evolution of the ionization fraction, x_e, of atoms, number density n, can be modeled in a simplified manner for the recombination of hydrogen, [22,23],

$$-\frac{dx_e}{dt}\bigg|_{\rm std} = C\left[a_c n x_e^2 - b_c(1-x_e)\exp\left(-\frac{\Delta B}{k_B T}\right)\right] \quad (1)$$

where a_c and b_c are the effective recombination and photoionization rates for principle quantum numbers ≥ 2, ΔB is the difference in binding energy between the 1st and 2nd energy levels and

$$C = \frac{1 + K\Lambda_{1s2s} n_{1s}}{1 + K(\Lambda_{1s2s} + b_c) n_{1s}}, \qquad K = \frac{\lambda_\alpha^3}{8\pi H(z)} \quad (2)$$

where λ_α is the wavelength of the single Ly-α transition from the $2p$ level, Λ_{1s2s} is the decay rate of the metastable $2s$ level, $n_{1s} = n(1-x_e)$ is the number of neutral ground state H atoms, and $H(z)$ is the Hubble expansion factor at a redshift z.

We include the possibility of extra photons at key wavelengths that would modify this recombination picture, namely, resonance (Ly-α) photons with number density, n_α, which promote electrons to the $2p$ level, and ionizing photons, n_i, [18,20,27,28]

$$\frac{dn_\alpha}{dt} = \varepsilon_\alpha(z) H(z) n, \qquad \frac{dn_i}{dt} = \varepsilon_i(z) H(z) n. \quad (3)$$

which leads to a modified evolution of the ionization fraction

$$-\frac{dx_e}{dt} = -\frac{dx_e}{dt}\bigg|_{\rm std} - C\varepsilon_i H - (1-C)\varepsilon_\alpha H. \quad (4)$$

Extra photon sources can be generated by a variety of mechanisms. A widely considered process is the decay or annihilation of massive particles [20,32–38]. The decay channel depends on the nature of the particles, and could, for example, include charged and neutral leptons, quarks or gauge bosons. These particles may then decay further, leading to a shower/cascade that could, amongst other products, generate a bath of lower energy photons that could interact with the primordial gas and cosmic microwave background. Interestingly these models, as well as injecting energy at recombination, $z \sim 1000$, boost the ionization fraction after recombination and can distort the ionization history of the universe at even later times, during galaxy formation and reionization $z \sim 5$–10 [9,39–42]. Other mechanisms include evaporation of black holes [27,43] or inhomogenities in baryonic matter [27].

We employ the widely used RECFAST code [24], in the COSMOMC package [44] modifying the code as in (4) to include two extra constant parameters, ϵ_α and ϵ_i. In addition to the ionizing sources, we assume a single, swift reionization epoch at a redshift $z_{\rm re}$.

In Fig. 1 we show the effect of additional resonance and ionizing radiation on the CMB TT, TE and EE spectra, in comparison to a fiducial best fit model to the WMAP 3-year data. From identical initial power spectra, the inclusion of additional resonance photons slightly boosts the ionization fraction at and after recombination, suppressing TT power at small scales, while the large scale EE spectra is largely unaffected. Ionizing photons significantly boost the ionization fraction post recombination and therefore as well as significantly suppressing TT power on small scales, they also can generate a boost in the large scale EE signal akin to an early partial reionization.

It is important to note that energy release at recombination could possibly lead to Sunyaev-Zel'dovich (SZ) distortions of the black body spectrum of the CMB. Change in temperature in the Rayleigh Jeans limit from SZ is given by $\Delta T/T = -2y$. From COBE/FIRAS [45] $y < 1.5 \times 10^{-5}$ at 95% c.l. We expect that energy injection as considered in this work to introduce a y parameter of the order (at most) of

$$y \approx 7.5 \times 10^{-3} \epsilon_\alpha (1+z)^{-3/2} \quad (5)$$

Therefore, around recombination $z \sim 1000$, we get

$$y \approx 2.36 \times 10^{-7} \epsilon_\alpha \quad (6)$$

Since, we are considering $\epsilon_\alpha \lesssim 0.5$ and $\epsilon_i \lesssim 0.01$, we expect the impact on the y parameter to be much smaller than the COBE/FIRAS constraint.

Moreover, those spectral distortions would appear at frequencies of hydrogen and helium recombination, around $\lambda \sim 0.1$ mm (see [46]), i.e. at frequencies not tested by the COBE-FIRAS experiment and strongly contaminated by thermal emission of galactic dust.

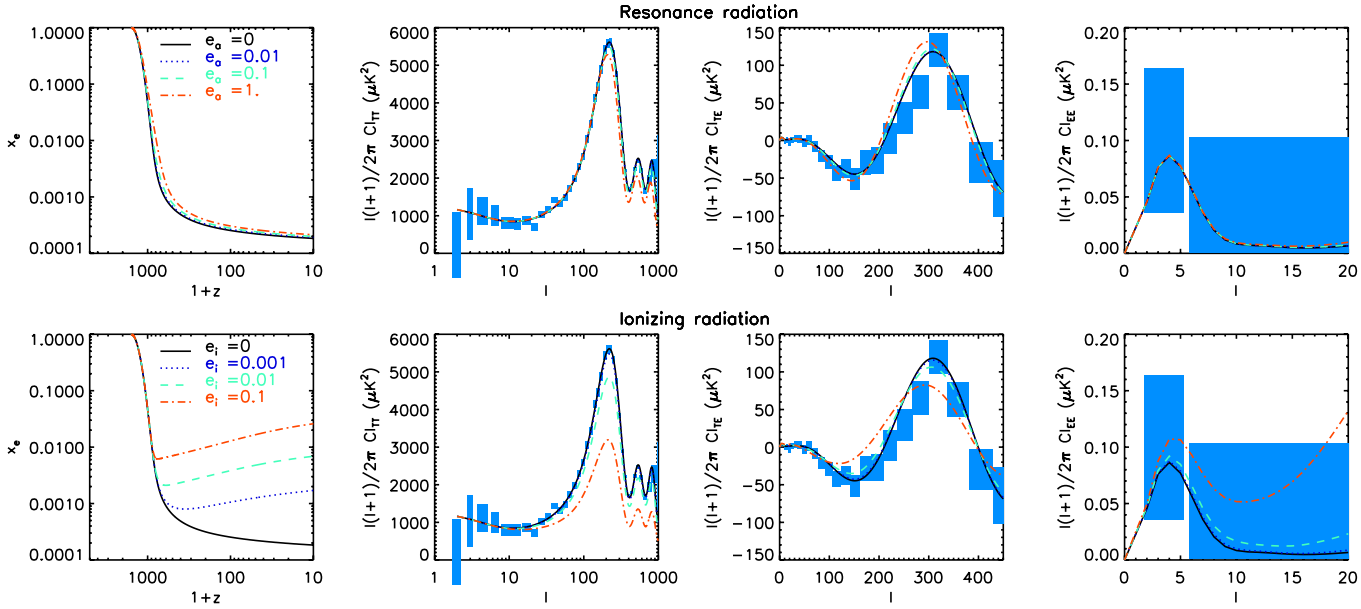

FIG. 1 (color online). (From left to right) The comparison of ionization fraction evolution, and TT (left), TE (center) and EE (right) CMB spectra comparing a best fit ΛCDM fiducial model to models with the same cosmological parameters but with additional resonance (top) and ionizing (bottom) radiation. WMAP binned data are shown as blue shaded regions.

III. LIKELIHOOD ANALYSIS

The method we adopt is based on the publicly available Markov Chain Monte Carlo package COSMOMC [44]. We sample the following dimensional set of cosmological parameters, adopting flat priors on them: the physical baryon and cold dark matter (CDM) densities, $\omega_b = \Omega_b h^2$ and $\omega_c = \Omega_c h^2$, the ratio of the sound horizon to the angular diameter distance at decoupling, θ_s, the scalar spectral index, n_s, and the optical depth to reionization, τ. As described in the previous section, we modify recombination by considering variations in the ε_α and ε_i parameters. Furthermore, we consider purely adiabatic initial conditions and we impose flatness. We also consider the possibility of having a tensor (gravity waves) component with amplitude r respect to scalar, a running of the spectral index $dn_s/d\ln k$ at $k = 0.002h^{-1}$ Mpc and a nonzero, degenerate, neutrino mass of energy density:

$$\Omega_\nu h^2 = \frac{\Sigma m_\nu}{92.5\ \mathrm{eV}} \tag{7}$$

Finally, we will also investigate the possibility of a dark energy equation of state, w, different from -1 but constant with redshift. The MCMC convergence diagnostics is done on 7 chains though the Gelman and Rubin "variance of chain mean"/"mean of chain variances" R statistic for each parameter. Our $1D$ and $2D$ constraints are obtained after marginalization over the remaining "nuisance" parameters, again using the programs included in the COSMOMC package. In addition to the WMAP data, we also consider the constraints on the real-space power spectrum of galaxies from the Sloan Digital Sky Survey (SDSS) [47]. We restrict the analysis to a range of scales over which the fluctuations are assumed to be in the linear regime ($k < 0.2h^{-1}$ Mpc). When combining the matter power spectrum with CMB data, we marginalize over a bias b considered as an additional nuisance parameter. Furthermore, we make use of the Hubble Space Telescope (HST) measurement of the Hubble parameter $H_0 = 100h$ km s^{-1} Mpc^{-1} [48] by multiplying the likelihood by a Gaussian likelihood function centered around $h = 0.72$ and with a standard deviation $\sigma = 0.08$. When considering dark energy models, we also include information from luminosity distance measurements of type Ia Supernovae from the recent analysis of [49]. Finally, we include a top-hat prior on the age of the universe: $10 < t_0 < 20$ Gyrs.

IV. RESULTS

Our main results are plotted in Fig. 2 where we show the 68% and 95% c.l. on the $n_s - \log_{10}(\epsilon_\alpha)$, $\sigma_8 - \log_{10}(\epsilon_\alpha)$, $n_s - \log_{10}(\epsilon_i)$ and $\sigma_8 - \log_{10}(\epsilon_i)$ plane. In the top portion of Fig. 2, we consider only the WMAP data (plus a prior on the Hubble parameter), while in the lower portion, we add SDSS. Let us first consider the case of WMAP alone. As we see, using this data set alone, we can put interesting new bounds on the recombination parameters. Marginalizing over the remaining, nuisance, parameters we indeed obtain $\log_{10}(\epsilon_\alpha) < -0.81$ and $\log_{10}(\epsilon_i) < -2.31$ at 95% c.l.

As suggested by Fig. 1, we find ionizing photons are better constrained with current data since the ionization fraction is significantly boosted at and beyond the onset of recombination. This results in a suppression of TT power

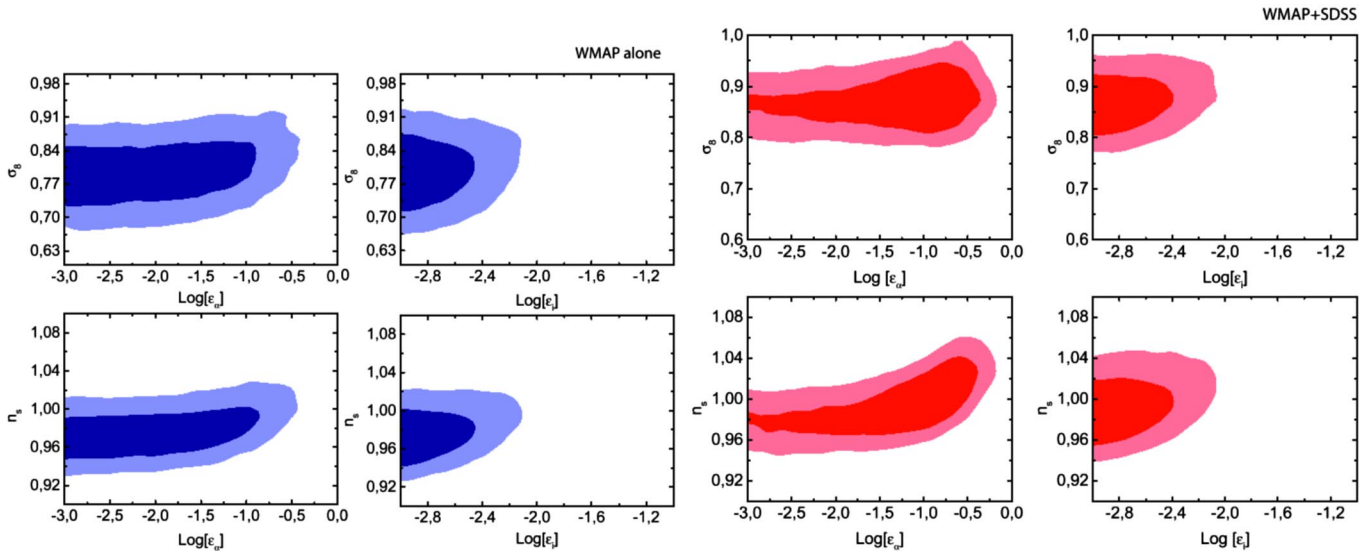

FIG. 2 (color online). The 68% and 95% likelihood contours in the n_s and σ_8 vs ε_α plane (left) and n_s and σ_8 vs ε_i (right). The analysis considers (top/blue) the 3-years WMAP data and a HST prior on the Hubble parameter, h, alone and (bottom/red) also including SDSS galaxy matter power spectrum data.

and boosting of EE power even on large scales, well constrained by WMAP data. Resonance photons have a more subtle effect only slightly increasing the ionization fraction after the onset of recombination. This leads to a suppression of small scale TT power but little effect on large scale EE. The constraints on both types of radiation should be noticeably improved therefore by future experiments, such as the planned PLANCK satellite, which better characterize small scale TT and EE power [28].

Moreover, there is a clear degeneracy between $\log_{10}(\epsilon_\alpha)$ and the spectral index n_s. Indeed, a modification of the recombination scheme allows us to suppress the amplitude of the peaks in the CMB power spectrum in a way similar to a later recombination but without altering the large-scale polarization signal. This changes in a drastic way the constraints on the scalar spectral index and σ_8. Marginalizing over the recombination parameters, we get $n_s = 0.978^{+0.032}_{-0.029}$ and $\sigma_8 = 0.80^{+0.08}_{-0.09}$ at 95% c.l. Those results should be compared with the constraints $n_s = 0.959^{+0.026}_{-0.027}$ and $\sigma_8 = 0.78^{+0.08}_{-0.07}$, again at 95% c.l., obtained using the same data set and priors but with standard recombination.

Including SDSS data, as is shown in the lower panel in Fig. 2, does not significantly improve our constraints on ε_α and ε_i. The SDSS power spectrum indeed prefers a higher value of the σ_8 parameter than WMAP. While the tension is not strong enough to provide any evidence for modified recombination, the constraints are lowered to $\log_{10}(\epsilon_\alpha) < -0.51$ for ε_α and almost stable to $\log_{10}(\epsilon_i) < -2.24$, for ε_i at 95% c.l. The constraints on n_s and σ_8 are also affected. Including SDSS we find $n_s = 0.994^{+0.040}_{-0.035}$ and $\sigma_8 = 0.87^{+0.07}_{-0.06}$ at 95% c.l.

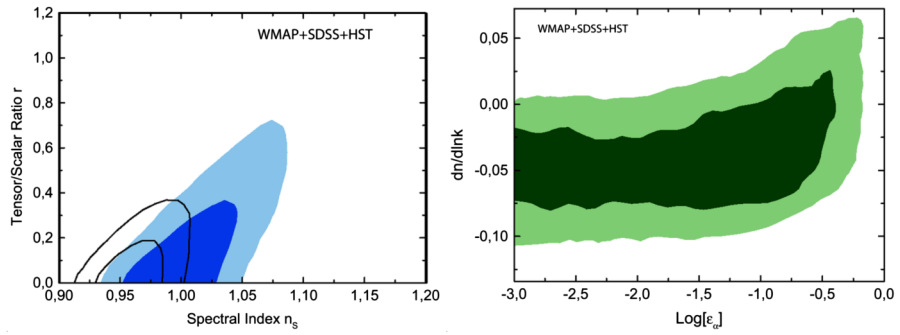

FIG. 3 (color online). The effect of a modified recombination scheme on inflationary parameters in a WMAP + SDSS analysis. In the top panel we plot the constraints in the $n_s - r$ plane. The filled contours (68% and 95%) are obtained after marginalization over extended recombination parameters while the empty contours assume standard recombination. In the bottom panel, we show the 68% and 95% likelihood contours in the $dn_s/d\ln k$ vs ε_α plane. Nonstandard recombination shifts the $\sim 1\sigma$ evidence for running in the standard case to a null result. Future evidence for running may be interpreted as evidence for a nonstandard recombination scheme.

Interestingly, we find that the constraints on other key parameters (τ or Ω_b) are robust to the modifications in the recombination scenario. It is interesting to extend the analysis to other inflationary parameters such as the amplitude of a tensor component r or a running of the spectra index $dn_s/d\ln k$. In Fig. 3 (top panel) we plot the 68% and 95% likelihood contours in the $n_s - r$ plane in the standard and in the generalized recombination case. As one can see, relaxing our knowledge about recombination strongly affects the final constraints: the scalar spectral index can be more consistent with $n_s > 1$ and the upper limit on the tensor component can be a factor 2 larger than in the standard case. As one can see from the bottom panel of Fig. 3 a degeneracy between ϵ_α and the running $dn_s/d\ln k$ is also present. Standard analyses prefer a negative running of the spectral index with significance slightly above 1σ (see [1]). This can be compensated for by a nonstandard recombination with $\epsilon_\alpha > 0.1$.

In Fig. 4, we report on the impact of nonstandard recombination on the equation of state parameter, w. We find an important degeneracy only with ϵ_α; allowing ϵ_α to vary enlarges the constraints on w towards more negative values. A future, combined, indication for $w < -1$ could, therefore, provide a hint of a nonstandard recombination process and one should be careful in interpreting it as evidence for a phantomlike dark energy component. In a more generalized recombination scenario, we find the constraints on w are relaxed to $w = -1.24^{+0.28}_{-0.44}$ at 95% c.l.

Finally, in Fig. 5, we report the constraints on neutrino masses. As one can see, nonstandard recombination also relaxes constraints on this parameter. We find that values as large as $\Sigma m_\nu \sim 1.2$ eV are consistent with the data, relaxing by ~50% the standard constraint $\Sigma m_\nu < 0.72$ eV (see e.g. [1,50]).

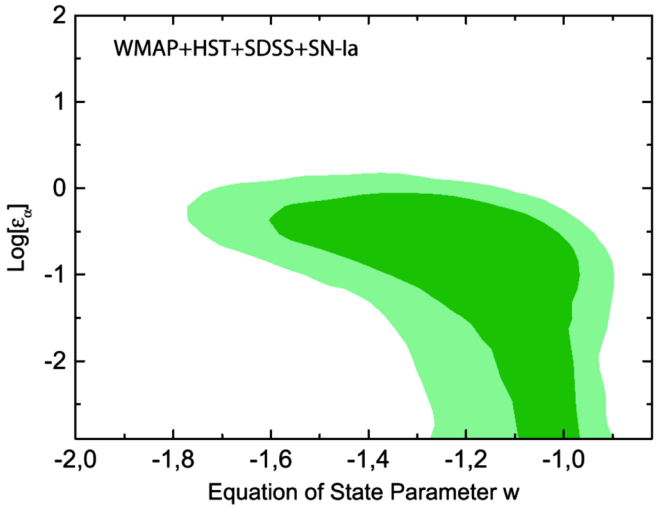

FIG. 4 (color online). The impact of a modified recombination scheme on constraining a constant dark energy equation of state, w. We show the 68% and 95% likelihood contours in the w vs ε_α plane from WMAP + SDSS + HST + SN-1a (see text). Nonstandard recombination relaxes the constraints towards more negative values for w.

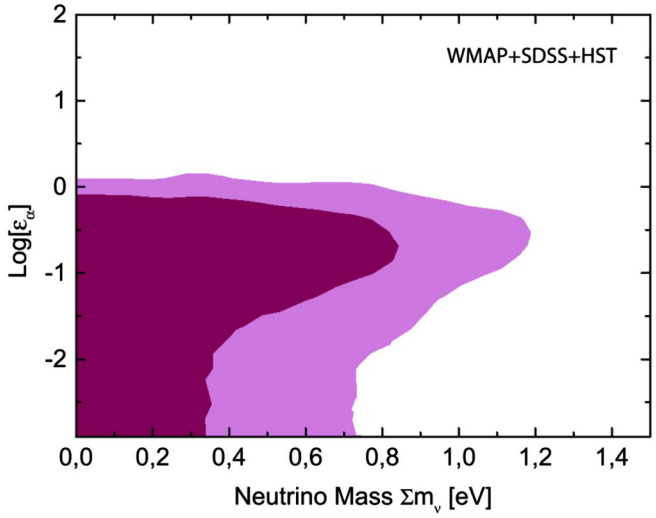

FIG. 5 (color online). The effect of a modified recombination scheme on constraining neutrino masses. We show the 68% and 95% likelihood contours in the Σm_ν vs ε_α plane from WMAP + SDSS + HST (see text). Nonstandard recombination relax the constraints towards larger masses.

V. CONCLUSIONS

In this paper, we update the upper bounds that can be placed on the contribution of extra Ly-α and ionizing photon-producing sources in light of the new WMAP data. We find that, adopting a simple parametrization using constant effective values for ε_α and ε_i, the WMAP data constraints $\log_{10}[\varepsilon_\alpha] < -0.5$ and $\log_{10}[\varepsilon_i] < -2.4$ at the 95% level. Physically motivated models for nonstandard recombination which generate ionizing and resonance radiation, like those based on primordial black hole or superheavy dark matter decay, remain feasible.

We find that a modified recombination scheme may affect the current WMAP constraints on inflationary parameters like the spectral index n_s and its running. In particular, if recombination is changed, Harrison-Zel'dovich spectra with $n_s = 1$, larger tensor modes and positive running are in agreement with observations. Moreover, constraints on particle physics parameters like the neutrino mass are also relaxed when nonstandard recombination is considered.

Are the corresponding restrictions obtained by the authors from the data of the CMB anisotropy in agreement with the COBE data in terms of the so called y-parameter?

Future observations in both temperature and polarization, such as those expected from the Planck satellite [28], will provide more precise small scale TT and EE measurements needed to more stringently test these models and, crucially, will reduce the dependency of other cosmological parameters on them.

ACKNOWLEDGMENTS

R. B.'s work is supported by NSF Grant Nos. AST-0607018 and PHY-0555216 and uses National Supercomputing (NCSA) resources under Grant No. TG-AST060029T.

[1] D. N. Spergel *et al.*, astro-ph/0603449.
[2] L. Page *et al.*, astro-ph/0603450.
[3] G. Hinshaw *et al.*, astro-ph/0603451.
[4] N. Jarosik *et al.*, astro-ph/0603452.
[5] L. Alabidi and D. H. Lyth, J. Cosmol. Astropart. Phys. 08 (2006) 013.
[6] H. Peiris and R. Easther, J. Cosmol. Astropart. Phys. 07 (2006) 002.
[7] D. Parkinson, P. Mukherjee, and A. R. Liddle, Phys. Rev. D **73**, 123523 (2006).
[8] C. Pahud, A. R. Liddle, P. Mukherjee, and D. Parkinson, Phys. Rev. D **73**, 123524 (2006).
[9] A. Lewis, astro-ph/0603753.
[10] U. Seljak, A. Slosar, and P. McDonaldJ. Cosmol. Astropart. Phys. 10 (2006) 014.
[11] J. Magueijo and R. D. Sorkin, astro-ph/0604410.
[12] R. Easther and H. Peiris, J. Cosmol. Astropart. Phys. 09 (2006) 010.
[13] W. H. Kinney, E. W. Kolb, A. Melchiorri, and A. Riotto, Phys. Rev. D **74**, 023502 (2006).
[14] C. Zunckel and P. G. Ferreira, astro-ph/0610597.
[15] R. Trotta, A. Riazuelo, and R. Durrer, Phys. Rev. D **67**, 063520 (2003).
[16] R. Bean, J. Dunkley, and E. Pierpaoli, Phys. Rev. D **74**, 063503 (2006).
[17] R. Keskitalo, H. Kurki-Suonio, V. Muhonen, and J. Valiviita, astro-ph/0611917.
[18] R. Bean, A. Melchiorri, and J. Silk, Phys. Rev. D **68**, 083501 (2003).
[19] S. Hannestad and R. J. Scherrer, Phys. Rev. D **63**, 083001 (2001).
[20] P. J. E. Peebles, S. Seager, and W. Hu, Astrophys. J. **539**, L1 (2000).
[21] S. Hannestad, Phys. Rev. D **60**, 023515 (1999); M. Kaplinghat, R. J. Scherrer, and M. S. Turner, Phys. Rev. D **60**, 023516 (1999); P. P. Avelino *et al.*, Phys. Rev. D **62**, 123508 (2000); R. Battye, R. Crittenden, and J. Weller, Phys. Rev. D **63**, 043505 (2001); P. P. Avelino *et al.*, Phys. Rev. D **64**, 103505 (2001); Landau, Harari, and Zaldarriaga, Phys. Rev. D **63**, 083505 (2001); C. J. A. Martins, A. Melchiorri, G. Rocha, R. Trotta, P. P. Avelino, and P. Viana, Phys. Lett. B **585**, 29 (2004).
[22] P. J. E. Peebles, Astrophys. J. **153**, 1 (1968).
[23] Ya. B. Zel'dovich, V. G. Kurt, and R. A. Sunyaev, Zh. Eksp. Teor. Fiz. **55**, 278 (1968) [Sov. Phys. JETP **28**, 146 (1969)].
[24] S. Seager, D. D. Sasselov, and D. Scott, Astrophys. J. **523**, L1 (1999).
[25] W. Hu, D. Scott, N. Sugiyama, and M. White, Phys. Rev. D **52**, 5498 (1995).
[26] U. Seljak, N. Sugiyama, M. White, M. Zaldarriaga, astro-ph/0306052.
[27] P. D. Naselsky and I. D. Novikov, Mon. Not. R. Astron. Soc. **334**, 137 (2002).
[28] A. G. Doroshkevich, I. P. Naselsky, P. D. Naselsky, and I. D. Novikov, Astrophys. J. **586**, 709 (2003).
[29] J. Chluba and R. A. Sunyaev, Astron. Astrophys. **446**, 39 (2006).
[30] J. Chluba, J. A. Rubino-Martin, and R. A. Sunyaev, astro-ph/0608242.
[31] W. Y. Wong and D. Scott, astro-ph/0610691.
[32] S. Sarkar and A. M. Cooper-Sarkar, Phys. Lett. **148B**, 347 (1983).
[33] D. Scott, M. J. Rees, and D. W. Sciama, Astron. Astrophys. **250**, 295 (1991).
[34] J. Ellis, G. Gelmini, J. Lopez, D. Nanopoulos, and S. Sarkar, Nucl. Phys. **B373**, 399 (1992).
[35] A. J. Adams, S. Sarkar, and D. W. Sciama, Mon. Not. R. Astron. Soc. **301**, 210 (1998).
[36] A. G. Doroshkevich and P. D. Naselsky, Phys. Rev. D **65**, 123517 (2002).
[37] P. D. Naselsky and L. Y. Chiang, Phys. Rev. D **69**, 123518 (2004).
[38] L. Zhang, X. L. Chen, Y. A. Lei, and Z. G. Si, Phys. Rev. D **74**, 103519 (2006).
[39] E. Pierpaoli, Phys. Rev. Lett. **92**, 031301 (2004).
[40] X. L. Chen and M. Kamionkowski, Phys. Rev. D **70**, 043502 (2004).
[41] N. Padmanabhan and D. P. Finkbeiner, Phys. Rev. D **72**, 023508 (2005).
[42] M. Mapelli, A. Ferrara, and E. Pierpaoli, Mon. Not. R. Astron. Soc. **369**, 1719 (2006).
[43] P. D. Naselsky and A. G. Polnarev, Sov. Astron. Lett. **13**, 167 (1987).
[44] A. Lewis and S. Bridle, Phys. Rev. D **66**, 103511 (2002).
[45] D. J. Fixsen, E. S. Cheng, J. M. Gales, J. C. Mather, R. A. Shafer, and E. L. Wright, Astrophys. J. **473**, 576 (1996).
[46] W. Y. Wong, S. Seager, and D. Scott, Mon. Not. R. Astron. Soc. **367**, 1666 (2006).
[47] M. Tegmark *et al.* (SDSS Collaboration), Astrophys. J. **606**, 702 (2004).
[48] W. L. Freedman *et al.*, Astrophys. J. **553**, 47 (2001).
[49] P. Astier *et al.*, Astron. Astrophys. **447**, 31 (2006).
[50] G. L. Fogli *et al.*, hep-ph/0608060.